Original Article

Co-cultured spheroids of human periodontal ligament mesenchymal stem cells and vascular endothelial cells enhance periodontal tissue regeneration

Kotaro Sano [a], Michihiko Usui [a, *], Yuki Moritani [a], Kohji Nakazawa [b], Tomoya Hanatani [a], Hisataka Kondo [c], Mitsushiro Nakatomi [d], Satoru Onizuka [a], Takanori Iwata [e], Tsuyoshi Sato [f], Akifumi Togari [c], Wataru Ariyoshi [g], Tatsuji Nishihara [g], Keisuke Nakashima [a]

[a] Division of Periodontology, Department of Oral Function, Kyushu Dental University, 2-6-1 Manazuru, Kokurakita-ku, Kitakyushu, Fukuoka 803-8580, Japan
[b] Department of Life and Environment Engineering, The University of Kitakyushu, 1-1 Hibikino, Wakamatsu-ku, Kitakyushu, Fukuoka, 808-0135, Japan
[c] Department of Pharmacology, School of Dentistry, Aichi-Gakuin University, 1-100 Kusumoto-cho, Chikusa-ku, Nagoya, Aichi 464-8650, Japan
[d] Division of Anatomy, Department of Health Improvement, Kyushu Dental University, 2-6-1 Manazuru, Kokurakita-ku, Kitakyushu, Fukuoka 803-8580, Japan
[e] Department of Periodontology, Graduate School of Medical and Dental Sciences, Tokyo Medical and Dental University, 1-5-45 Yushima, Bunkyo-ku, Tokyo 113-8510, Japan
[f] Department of Oral and Maxillofacial Surgery, Saitama Medical University, 38 Morohongo, Moroyama-machi, Iruma-gun, Saitama 350-0495, Japan
[g] Division of Infection and Molecular Biology, Department of Health Improvement, Kyushu Dental University, 2-6-1 Manazuru, Kokurakita-ku, Kitakyushu, Fukuoka 803-8580, Japan

ARTICLE INFO

ABSTRACT

Introduction: Human periodontal ligament mesenchymal stem cells (hPDLMSCs) have been known that they play important roles in homeostasis and regeneration of periodontal tissues. Additionally, spheroids are superior to monolayer-cultured cells. We investigated the characteristics and potential of periodontal tissue regeneration in co-cultured spheroids of hPDLMSCs and human umbilical vein endothelial cells (HUVECs) *in vitro* and *in vivo*.
Methods: Co-cultured spheroids were prepared with cell ratios of hPDLMSCs: HUVECs = 1:1, 1:2, and 2:1, using microwell chips. Real-time polymerase chain reaction (PCR) analysis, Enzyme-Linked Immuno Sorbent Assay (ELISA), and nodule formation assay were performed to examine the properties of co-cultured spheroids. Periodontal tissue defects were prepared in the maxillary first molars of rats and subjected to transplantation assay.
Results: The expression levels of stemness markers, vascular endothelial growth factor (*VEGF*), osteogenesis-related genes were up-regulated in co-cultured spheroids, compared with monolayer and spheroid-cultured hPDLMSCs. The nodule formation was also increased in co-cultured spheroids, compared with monolayer and spheroid cultures of hPDLMSCs. Treatment with co-cultured spheroids enhanced new cementum formation after 4 or 8 weeks of transplantation, although there was no significant difference in the new bone formation between co-cultured spheroids and hPDLMSC spheroids.
Conclusions: We found that co-cultured spheroids enhance the periodontal tissue regeneration. Co-cultured spheroids of hPDLMSCs and HUVECs may be a useful therapy that can induce periodontal tissue regeneration.

---

* Corresponding author. Division of Periodontology, Department of Oral Function, Kyushu Dental University, 2-6-1 Manazuru, Kokurakita-ku, Kitakyushu, Fukuoka, 803-8580, Japan.
E-mail address: r12usui@fa.kyu-dent.ac.jp (M. Usui).
Peer review under responsibility of the Japanese Society for Regenerative Medicine.

1. Introduction

Periodontitis is chronic inflammatory disease of tooth-supporting tissue, and the progression of periodontal disease could finally lead to tooth loss in adults [1]. Several regenerative strategies, such as cytokine therapies, have been tested to reconstruct the tooth-supporting structures lost during progression of the disease [2,3]. However, the complexity of periodontal tissue makes it difficult to completely regenerate the periodontal tissue [4].

On the basis of recent progress in tissue engineering, mesenchymal stem cells (MSCs) are useful for tissue regeneration because they have the potential to differentiate into multilineages [5,6]. We focused on human periodontal ligament mesenchymal stem cells (hPDLMSCs), which have been reported to have characteristics of MSCs and multilineage differentiation abilities; these lineages include osteoblasts, adipocytes, and chondrocytes, when hPDLMSCs are grown in the appropriate induction medium [7−9]. hPDLMSCs also have the ability to differentiate into osteoblasts and cementoblast-like cells in an appropriate *in vivo* environment [7,10]. The periodontal ligament cell sheet, which is prepared by the cell engineering technology, shows a good regenerative potential in animal experiments [11,12]. Thus, hPDLMSCs have been proven to be useful in regenerating lost periodontal tissue.

Generally, MSCs are prepared by traditional two-dimensional (2D) culture as monolayers. Proteolytic enzyme treatments are performed to collect the cells cultured two-dimensionally in the culture dish. This process inflicts damage on cell−extracellular matrix interaction, which leads to the impairment of cell function [13]. To overcome the disadvantages of 2D culture system, several methods of three-dimensional (3D) cell culture have been studied; culture in a low-adherence 96-well plate, and rotational culture system [14,15]. Three-dimensional culture systems can reproduce the *in vivo* condition, compared with 2D culture systems [16]. In addition, the 3D arrangement of cells provides superior cell−cell interactions, improved extracellular matrix organization, and production of various growth factors [17−21]. Spheroids are multicellular spherical clusters formed by 3D self-aggregation [22]. MSCs cultured in a spheroid culture system are more effective for induction of MSC differentiation than MSCs cultured in a monolayer culture system, and the spheroid structure contributes to the augmentation of MSC bioactivities and the optimization for therapeutic efficiency [23]. We have demonstrated utilization of spheroids that were formed with specially prepared microchips (diameter: 500 μm) that had been modified with polyethylene glycol (PEG) to make them nonadhesive to cells [24,25]. In this system, spheroids can be harvested from the microwells without requiring proteolytic enzymes. Moreover, this culture system allows spheroids to be prepared easily, compared with conventional spheroid formation methods.

We found out that spheroid cultures of hPDLMSCs enhanced the pluripotency and the regenerative ability of bone tissue, compared with monolayer cultures of hPDLMSCs [17]. A study focusing on coculture system reports that the hPDLMSC−human umbilical vein endothelial cells (HUVECs) co-cultured cell sheet exhibited significantly high levels of osteogenesis-related markers, compared with hPDLMSC cell sheet [26]. Another study showed that the hPDLMSC−HUVEC−hPDLMSC cell sheet was effective for regeneration of the periodontal tissues in the transplantation assay [27]. Therefore, in this study, we investigated the characteristics of co-cultured spheroids containing hPDLMSCs and HUVECs, and evaluated the periodontal tissue regeneration by transplanting co-cultured spheroids into periodontal tissue defects.

2. Methods

2.1. Animals

Forty male Sprague−Dawley (SD) rats (age 7 weeks; CLEA Japan, Tokyo, Japan) were employed in this study. All study protocols and procedures were approved by the Animal Care and Use Committee, Kyushu Dental University (Protocol #16-027). This study was conducted in accordance with ARRIVE (Animal Research: Reporting In Vivo Experiments) guidelines and the National Institutes of Health guide for care and use of Laboratory animals.

2.2. Cell isolation and culture

As described previously [7,9,28], hPDLMSCs were obtained from the human periodontal ligament (hPDL) of wisdom teeth freshly extracted from healthy subjects who were treated for impaction. We obtained informed consents from all subjects. This study protocol was approved by the Kyushu Dental University Ethics Committee (Protocol #14-021), and all procedures complied with Declaration of Helsinki and the guidelines provided by Kyushu Dental University. The extracted wisdom teeth were washed five times with Phosphate-Buffered Saline (PBS) (Thermo Fisher Scientific, Waltham, MA, USA) containing antibiotics (100 U/mL penicillin and 100 μg/mL streptomycin; Wako Pure Chemicals, Osaka, Japan). The hPDL tissue was removed from the middle of the root surface and subsequently incubated in digestion solution containing alpha minimal essential medium (α-MEM) (Thermo Fisher Scientific) with collagenase Type 1 (1 mg/mL; Wako) and dispase (1200 PU/ml; Wako) at 37 °C for 60 min in continuous agitation. Following the enzymatic digestion, the cell suspensions were passed through a cell strainer (pore size, 70 μm) (BD Falcon, Bedford, MA, USA) to remove debris. Then, cell suspensions were poured onto 100 mm tissue culture dishes (Iwaki, Shizuoka, Japan) and cultured in 10 mL growth medium; α-MEM containing 10% fetal bovine serum (FBS) (Biosera, Nuaillé, France), 100 U/mL penicillin (Wako) and 100 μg/mL streptomycin (Wako). The medium was replaced every 4 days. Colony-forming hPDLMSCs were harvested and subcultured when they became confluent. hPDLMSCs had been passaged fewer than five times were used for the first experiments. We confirmed hPDLMSCs have osteogenesis, adipogenesis and chondrogenesis in the osteogenic, adipogenic and chondrogenic induction medium (data not shown).

HUVECs (ATCC Cat# CRL-1730) were purchased from American Type Culture Collection (Manassas, VA, USA) and cultured in endothelial cell growth medium-2 (EGM-2) (Lonza, Basel, Switzerland). The medium was replaced every 3 days. HUVECs passaged less than five times were employed for the first experiments.

2.3. Co-cultured spheroid formation

Microwell chips fabricated for the formation of spheroid were prepared as previously described [24,25]. In brief, the surface of the microwell with 500 μm diameter and 500 μm depth was coated with a layer of platinum, and then PDMS (polydimethylsiloxane) frame surrounding all microwells was set on the center of the microwell chip. The chip was modified with 5 mM PEG to get it unattached to cells, and placed in a 35 mm culture dish (BD Falcon) filled with 2 mL of mixed α-MEM and EGM-2. For preparation of co-cultured spheroids, mixtures of 4.0×10^5 cells with hPDLMSCs: HUVECs at ratios of 1:1, 1:2, or 2:1 were seeded in a PDMS frame. Since the microwell chip is designed as 200 wells/chip, 200 homogeneous spheroids (2000 cells/spheroid) are formed from this cell suspension [17]. Three hours after cell seeding, the dish with

PDMS frame removed was tilted and incubated with 5% CO_2 at 37 °C for 3 days. Co-cultured spheroids, hPDLMSC spheroids, and HUVEC spheroids were observed using a biological microscope (BX50) (Olympus, Tokyo, Japan) at 3 days after seeding.

2.4. Quantitative real-time PCR

Real-time reverse-transcription polymerase chain reaction (RT-PCR) was performed according to the previous report [29]. Total RNA was isolated from co-cultured spheroids (hPDLMSCs: HUVECs = 1:1, 1:2, and 2:1), hPDLMSC spheroids, and monolayer cultures of hPDLMSCs and HUVECs at 3 days post-seeding with an RNeasy Mini Kit (Qiagen, Hilden, Germany). Complementary DNA (cDNA) was generated by reverse transcription from RNA using a High-Capacity RNA-to-cDNA™ Kit (Thermo Fisher Scientific). Quantitative real-time RT-PCR was carried out using FAST SYBR® Green Master Mix (Applied Biosystems) in triplicate with the StepOnePlus™ Real-time PCR System (Applied Biosystems, Carlsbad, CA, USA). Table 1 lists the primer sequences used to detect PCR products. Relative gene expression was quantified with the comparative CT method. Total cDNA expression level of each sample was normalized using the *GAPDH* specific primers.

2.5. ELISA

The culture supernatants from co-cultured spheroids (hPDLMSCs: HUVECs = 1:1, 1:2, and 2:1), hPDLMSC spheroids, and monolayer cultures of hPDLMSCs and HUVECs at 3 days after seeding were harvested, and vascular endothelial growth factor (VEGF) protein levels in supernatants were tested using Human VEGF Quantikine ELISA Kit (R&D Systems) following the manufacturer's instructions.

2.6. Nodule formation

Induction of osteogenic differentiation and the alizarin red staining procedure were performed in accordance with a previously published protocol [17]. For osteogenic differentiation, 4.0×10^3 monolayer-cultured hPDLMSCs, two hPDLMSC spheroids (2000 cells/spheroid), or two co-cultured spheroids (hPDLMSCs: HUVECs = 1:1, 1:2, and 2:1) (2000 cells/spheroid) were seeded in a 48-well cell culture plate (Iwaki) as monolayer conditions in culture medium, and the culture medium was changed to hMSC Osteogenic Induction Medium (OIM) containing dexamethasone, L-

Table 1
Primer sequences for real-time reverse-transcription polymerase chain reaction analyses.

Genes	Sequences of primers
GAPDH	F: 5′-GAAGGTGAAGGTCGGAGTC-3′
	R: 3′-GAAGATGGTGATGGGATTTC-5′
OCT4	F: 5′-AGCAAAACCCGGAGGAGT-3′
	R: 3′-CCACATCGGCCTGTGTATATC-5′
NANOG	F: 5′-TGAACCTCAGCTACAAACAG-3′
	R: 3′-TGGTGGTAGGAAGAGTAAAG-5′
ALP	F: 5′-ACGTGGCTAAGAATGTCATC-3′
	R: 3′-CTGGTAGGCGATGTCCTTA-5′
BSP	F: 5′-AAAACGAAGAAGCGAAGC-3′
	R: 3′-TATTCATTGACGCCCGTGTA-5′
RUNX2	F: 5′-AACCCTTAATTTGCACTGGGTCA-3′
	R: 3′-CAAATTCCAGCAATGTTTGTGCTAC-5′
COL1	F: 5′-AGGGCTCCAACGAGATCGAGATCCG-3′
	R: 3′-TACAGGAAGCAGACAGGGCCAACGTCG-5′
VEGF	F: 5′-CCGCAGACGTGTAAATGTTCCT-3′
	R: 3′-CGGCTTGTCACATCTGCAAGTA-5′

glutamine, ascorbate, penicillin/streptomycin, mesenchymal cell growth supplement, and β-glycerophosphate (Lonza) when cells reached confluent. At 7, 10, 13, 17, and 21 days after medium change, the cells were fixed with a 4% paraformaldehyde phosphate buffer (Wako). Deposited calcium was stained with a 1% alizarin red solution (Wako) and quantified using ImageJ (National Institutes of Health, Bethesda, MD, USA). The alizarin red positive colony ratio was calculated from the bottom area of the wells and the area of nodules stained with alizarin red.

2.7. Transplantation of co-cultured spheroids in rat periodontal tissue defects

Forty SD rats were anesthetized with an intraperitoneal administration of three types of mixed anesthetic agents containing medetomidine hydrochloride (0.15 mg/kg) (Wako), midazolam (2 mg/kg) (Dormicum®, Astellas Pharma, Tokyo, Japan) and butorphanol tartrate (2.5 mg/kg) (Vetorphale®, Meiji Seika Pharma, Tokyo, Japan). The gingiva of the bilateral maxillary first molars was incised, and the full-thickness gingival flap of the palatal side was elevated. The furcation defects (buccopalatal depth, 1.3 mm; horizontal depth, 1.0 mm) were created at the mesial furcation by removing the alveolar bone, periodontal ligament, and root cementum using a dental bur (NTI-Kahla, Kahla, Germany). The reference notches were surgically created in both mesiobuccal and palatal roots to point at the bottom of the defects. Defects were (1) left untreated (sham operation; n = 3) and filled with (2) Matrigel® (Corning, NY, USA; as a carrier; n = 3); (3) monolayer-cultured hPDLMSCs (4.0×10^5 cells) with Matrigel® (n = 5); (4) monolayer-cultured HUVECs (4.0×10^5 cells) with Matrigel® (n = 5); (5) 2.0×10^3 hPDLMSC spheroids (2000 cells/spheroid) with Matrigel® (n = 6); (6) 2.0×10^3 co-cultured spheroids (2000 cells/spheroid) with hPDLMSCs: HUVECs at a ratio of 1:1, conbined with Matrigel® (n = 6); (7) 2.0×10^3 co-cultured spheroids (2000 cells/spheroid) with hPDLMSCs: HUVECs at a ratio of 1:2, conbined with Matrigel® (n = 6); (8) 2.0×10^3 co-cultured spheroids (2000 cells/spheroid) with hPDLMSCs: HUVECs at a ratio of 2:1, conbined with Matrigel® (n = 6). Cells were suspended into 10 μl of Matrigel® and then transplanted into the defects. After transplantation, the gingival flap was repositioned and closed with 7-0 silk sutures (Mani, Tochigi, Japan).

2.8. Microcomputed tomography analysis

At 4 or 8 weeks postoperatively, all rats were sacrificed by anesthetic overdose. Subsequently, the maxillae were removed, and healing of the periodontal defects was examined using three-dimensional micro X-Ray computed tomography (3D μCT) and TRI/3D-BON (Ratoc System Engineering, Tokyo, Japan). We measured the length of the bone in sliced CT images, in accordance with a previously published procedure [30]. We drew two tangent lines at the mesial and distal sides of the palatal and mesiobuccal roots. A perpendicular line on the distal tangent line was drawn at the center of the furcation. On the perpendicular line, the amount of horizontal bone filling was calculated as follows using length as shown in Fig. 4 (**a**): the rate of bone filling = (a/a+b) × 100. Furthermore, the bone volume fraction (BV/TV) was measured from the root apex to the mesial furcation of the maxillary first molar between the mesiobuccal and palatal roots.

2.9. Histological analysis and morphometric assessment

The maxillae were dissected and fixed with a 4% paraformaldehyde phosphate buffer (Wako) for 3 days. The maxilla blocks were decalcified in Morse's solution at 4 °C for 4 days,
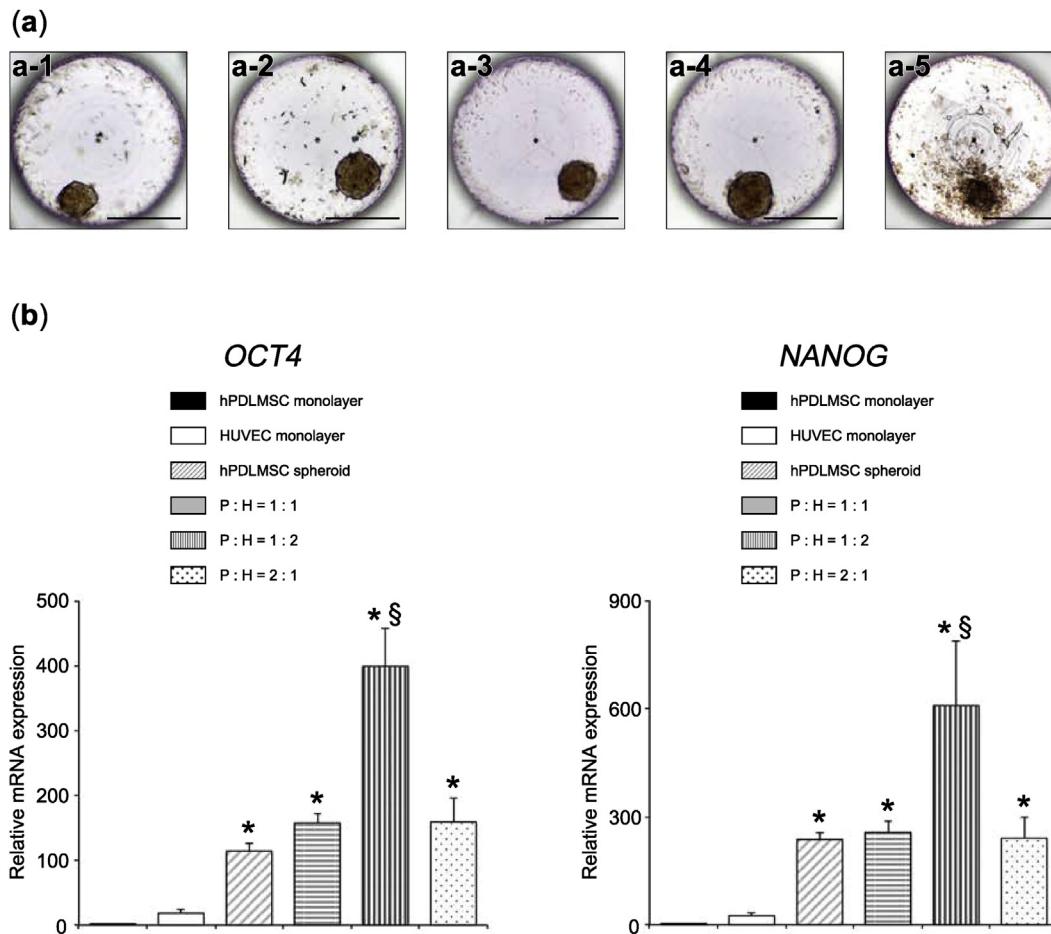
(a)

(b)

Fig. 1. Characteristics of co-cultured spheroids. (**a**) Microscopic images of spheroids. All spheroids were prepared at a density of 2000 cells/well, using microwell chips at 3 days post-seeding. Co-cultured spheroid (cell ratio of hPDLMSCs: HUVECs = 1:1) (**a-1**). Co-cultured spheroid (cell ratio of hPDLMSCs: HUVECs = 1:2) (**a-2**). Co-cultured spheroid (cell ratio of hPDLMSCs: HUVECs = 2:1) (**a-3**). hPDLMSC spheroid (**a-4**). HUVEC spheroid (**a-5**). Scale bar = 200 μm. (**b**) Expression of stemness markers in co-cultured spheroids (1:1, 1:2, and 2:1), hPDLMSC spheroids, hPDLMSCs and HUVECs grown in monolayer culture on day 3. The values were normalized to *GAPDH* expression. *$p < 0.05$ (compared with monolayer cultures of hPDLMSCs). §$p < 0.05$ (compared with hPDLMSC spheroids).

followed by dehydration and paraffin embedding. Serial tissue sections with thickness of 8 μm were cut out and stained with haematoxylin-eosin (H&E). The area of newly formed bone and the rate of new cementum length were measured using ImageJ, as described previously [31,32]. The area of newly formed bone was estimated as the ratio of the area surrounded by the top of the newly formed bone and reference notches on the mesiobuccal and palatal root surfaces. The newly formed cementum was defined as the portion of cementum that was found on the crown side above the notches, and in which Sharpey's fibers were inserted. The rate of new cementum length was defined as the ratio of the new cementum length formed on the root surface facing the defect to the root surface length from notch to notch. Regarding the cell transplant groups, Azan staining was used to confirm the running of Sharpey's fibers. Paraffin-embedded samples were stained with 0.1% Azocarmin G (Wako), Aniline alcohol (Wako), Acetic acid-ethanol (Wako), 5% Phosphotungstic acid (Wako), and Aniline Blue-Orange G Solution (Wako).

2.10. Statistical analysis

Data are expressed as mean ± standard deviation and all experiments were repeated in triplicate. Statistical differences between groups were assessed by Student's *t*-test or Bonferroni correction. Differences with $p < 0.05$ were considered significant.

3. Results

3.1. Co-cultured spheroid formation

As described previously [17], spheroids of hPDLMSCs alone (hPDLMSC spheroids) were formed from hPDL cells, using micro-well chips (Fig. 1 (**a-4**)). We examined the generation of co-cultured spheroids from hPDLMSCs and HUVECs, as well as spheroids of HUVECs alone (HUVEC spheroids). Co-cultured spheroids of three cell ratios (hPDLMSCs: HUVECs = 1:1, 1:2, and 2:1) were successfully prepared. According to microscopy observations, co-cultured spheroids were formed and could retain their original shapes, even when dropped from the microwells by pipetting (Fig. 1 (**a-1, 2, 3**)). HUVEC spheroids could be formed in microwells; however, the outline of HUVEC spheroids was irregular compared with that of the other spheroids (Fig. 1 (**a-5**)). Moreover, HUVEC spheroids collapsed during pipetting and could not be used for the following assay. In measurements of the diameter of spheroids 3 days after seeding on microwell chips, the average diameters of co-cultured spheroids (hPDLMSCs: HUVECs = 1:1, 1:2, and 2:1) and hPDLMSC spheroids were 102.2 μm, 105.9 μm, 116.2 μm, and 134.9 μm,

respectively, and no significant difference was observed in the size of spheroids.

3.2. Enhancement of stemness in co-cultured spheroids

We examined the expression of octamer-binding transcription factor 4 (OCT4) and NANOG in co-cultured spheroids by real-time RT-PCR. These transcription factors are considered to be essential for maintaining stemness and self-renewal of various stem cells. It was revealed that OCT4 and NANOG were significantly higher in 1:2 (hPDLMSCs: HUVECs) co-cultured spheroids, compared with monolayer cultures of hPDLMSCs and hPDLMSC spheroids (Fig. 1 (**b**)).

3.3. Osteogenic properties of co-cultured spheroids

To investigate the osteogenic potential of co-cultured spheroids, co-cultured spheroids cultured in OIM were assayed for nodule formation using alizarin red S stain. The results of alizarin red-positive nodules indicated an enhanced osteogenic potential of spheroid-cultured hPDLMSCs compared with monolayer-cultured hPDLMSCs, as shown by Fig. 2 (**a**), (**b**). The area of stained extracellular calcification was significantly greater in co-cultured spheroids (hPDLMSCs: HUVECs = 1:2 and 2:1 on day 13 and = 2:1 on day 17) than in hPDLMSC spheroids, however, there was no significant difference between co-cultured spheroids and hPDLMSC spheroids on day 21 (Fig. 2 (**a**), (**b**)). These data suggested that co-cultured spheroids induced calcification in an early period.

To explore whether osteogenesis-related genes are induced in OIM-treated co-cultured spheroids, the expression levels of alkaline phosphatase (ALP), bone sialoprotein (BSP), runt-related transcription factor 2 (RUNX2), and type 1 collagen (COL1) were measured by real-time RT-PCR. Spheroid culture of hPDLMSCs alone or co-culture of hPDLMSCs and HUVECs augmented the mRNA expression of ALP (hPDLMSCs alone and hPDLMSCs: HUVECs = 1:1 and 1:2 on day 7), BSP (hPDLMSCs: HUVECs = 1:2 on day 14), RUNX2 (hPDLMSCs alone on day 10 and hPDLMSCs: HUVECs = 1:1 on day 10 and = 1:2 on day 14), and COL1 (hPDLMSCs alone on day 10 and hPDLMSCs: HUVECs = 1:2 and 2:1 on day 10 and = 1:2 on day 14), compared with monolayer-cultured hPDLMSCs in each genes (Fig. 2 (**c**)). Moreover, real-time RT-PCR results revealed that co-culture of hPDLMSCs and HUVECs significantly enhanced the mRNA expression of ALP (hPDLMSCs: HUVECs = 1:1 and 2:1 on day 10), BSP (hPDLMSCs: HUVECs = 1:2 on day 14), RUNX2 (hPDLMSCs: HUVECs = 1:1 on day 10 and = 1:2 on day 14), and COL1 (hPDLMSCs: HUVECs = 1:2 on day 14), compared with spheroids of hPDLMSCs alone in each genes (Fig. 2 (**c**)). These findings suggested that co-cultured spheroids enhanced the osteogenic potential through the up-regulation of osteogenesis-related genes.

3.4. Preparation of periodontal defects and transplantation assay

We established periodontal defects at the mesial furcation of the maxillary first molars of the rats, and performed a transplantation assay to investigate the periodontal regeneration potential of co-cultured spheroids. The protocol and groups are shown in Fig. 3 (**a**). hPDLMSCs/HUVECs were seeded on microwell chips, and spheroids were collected 3 days later. The numbers of cells were set at 4.0×10^5 for monolayers (hPDLMSCs, HUVECs) and 2.0×10^3 for spheroids (co-cultured, hPDLMSC) (2000 cells/spheroid). We transplanted monolayer-cultured hPDLMSCs, HUVECs, hPDLMSC spheroids, or co-cultured spheroids (cell ratio of hPDLMSCs: HUVECs = 1:1, 1:2, and 2:1) into the rat periodontal tissue defects prepared at the mesial furcations of the maxillary first molars using

Matrigel®. Sacrifices were performed at 4 or 8 weeks after the operation. Fig. 3 (**b**) shows a macroscopic view of the oral cavity (focused on the upper jaw area) of the rat, and Fig. 3 (**c**) indicates the surgical condition of the maxillary first molar in the right side. Fig. 3 ((**d**); before defect creation) and 3 ((**e**); after defect creation) are enlarged images of the surgical site.

3.5. Analysis with 3D micro X-Ray computed tomography after transplantation

We assessed the rate of bone filling and BV/TV, as described in Fig. 4 (**a**), (**d**). In the co-cultured spheroids (hPDLMSCs: HUVECs = 1:1, 1:2, and 2:1) and hPDLMSC spheroids transplanted groups, the rate of bone filling was greater than that of sham group at 4 and 8 weeks after the operation. In contrast, there was no significant difference between the rate of bone filling treated with co-cultured spheroids (hPDLMSCs: HUVECs = 1:1, 1:2, and 2:1) and the rate of bone filling treated with spheroids of hPDLMSCs alone at 4 and 8 weeks postoperatively (Fig. 4 (**b**), (**c**)). BV/TV treated with co-cultured spheroids (hPDLMSCs: HUVECs = 1:1, 1:2, and 2:1) and hPDLMSC spheroids at 4 and 8 weeks postoperatively was significantly enhanced compared with sham group. At 8 week after the operation, the 1:1 and 2:1 (hPDLMSCs: HUVECs) co-cultured spheroids significantly increased BV/TV, compared with monolayer-cultured hPDLMSCs. Similar to the rate of bone filling, there was no significant difference between BV/TV treated with hPDLMSC spheroids and BV/TV treated with co-cultured spheroids (hPDLMSCs: HUVECs = 1:1, 1:2, and 2:1) at 4 and 8 weeks postoperatively (Fig. 4 (**e**), (**f**)). These data suggested that treatment with spheroids (co-cultured, hPDLMSC) enhanced new bone formation compared with sham, career (Matrigel®), and monolayer-cultured HUVECs treatments, although co-cultured spheroids have little effect on bone formation compared with spheroids of hPDLMSCs alone.

3.6. Histological evaluation of rat periodontal tissues after transplantation

Histological analysis was performed to investigate whether co-cultured spheroids could regenerate alveolar bone, as well as periodontal ligament and cementum. At 4 and 8 weeks after the operation, the sham and Matrigel® treatments hardly induced new bone, whereas in the co-cultured spheroids (hPDLMSCs: HUVECs = 1:1, 1:2, and 2:1) and hPDLMSC spheroids transplanted groups, new bone at the furcation was greater than in the groups transplanted with monolayer-cultured hPDLMSCs and HUVECs (Fig. 5 (**a**)). At 8 weeks postoperatively, the area of newly formed bone was significantly enhanced in the groups transplanted with co-cultured spheroids (hPDLMSCs: HUVECs = 1:1, 1:2, and 2:1) and hPDLMSC spheroids, compared with the groups received sham and monolayer-cultured hPDLMSCs treatments. However, there was no significant difference between co-cultured spheroid and hPDLMSC spheroid transplanted groups (Fig. 5 (**b**), (**c**)). Quantitative analysis of new cementum length elucidated that the rate of new cementum length in the co-cultured spheroids (hPDLMSCs: HUVECs = 1:1, 1:2, and 2:1) groups was significantly higher than that in hPDLMSCs spheroid group (Fig. 5 (**d**), (**e**)). We can observe Sharpey's fibers which are the part of the periodontal ligament inserted into the cementum-like layer in co-cultured spheroids (hPDLMSCs: HUVECs = 1:1, 1:2, and 2:1) and hPDLMSC spheroid groups, upon staining with H&E (Fig. 6 (**b**); high magnification), according to the images observed at the site shown in Fig. 6 (**a**). In the sections stained with Azan, which enables distinct identification of collagen fibers, Sharpey's fibers were also observed entering into the cementum-like structure in the tissue sections of co-cultured
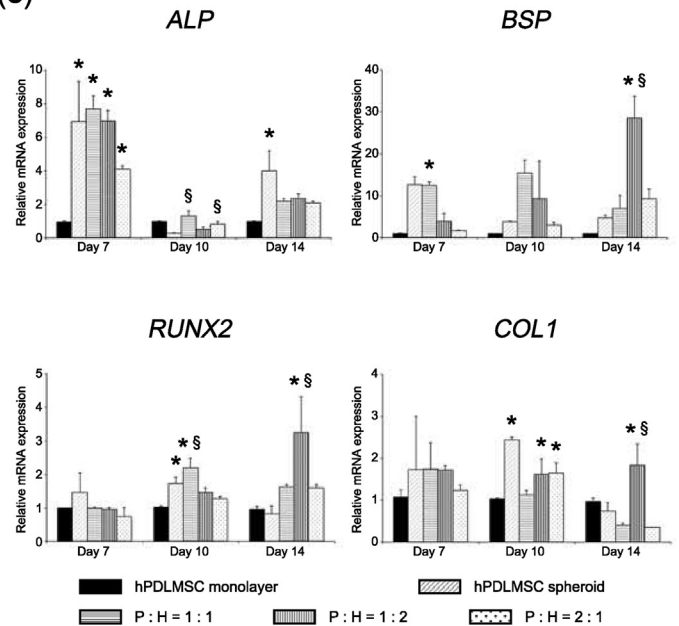
(a)
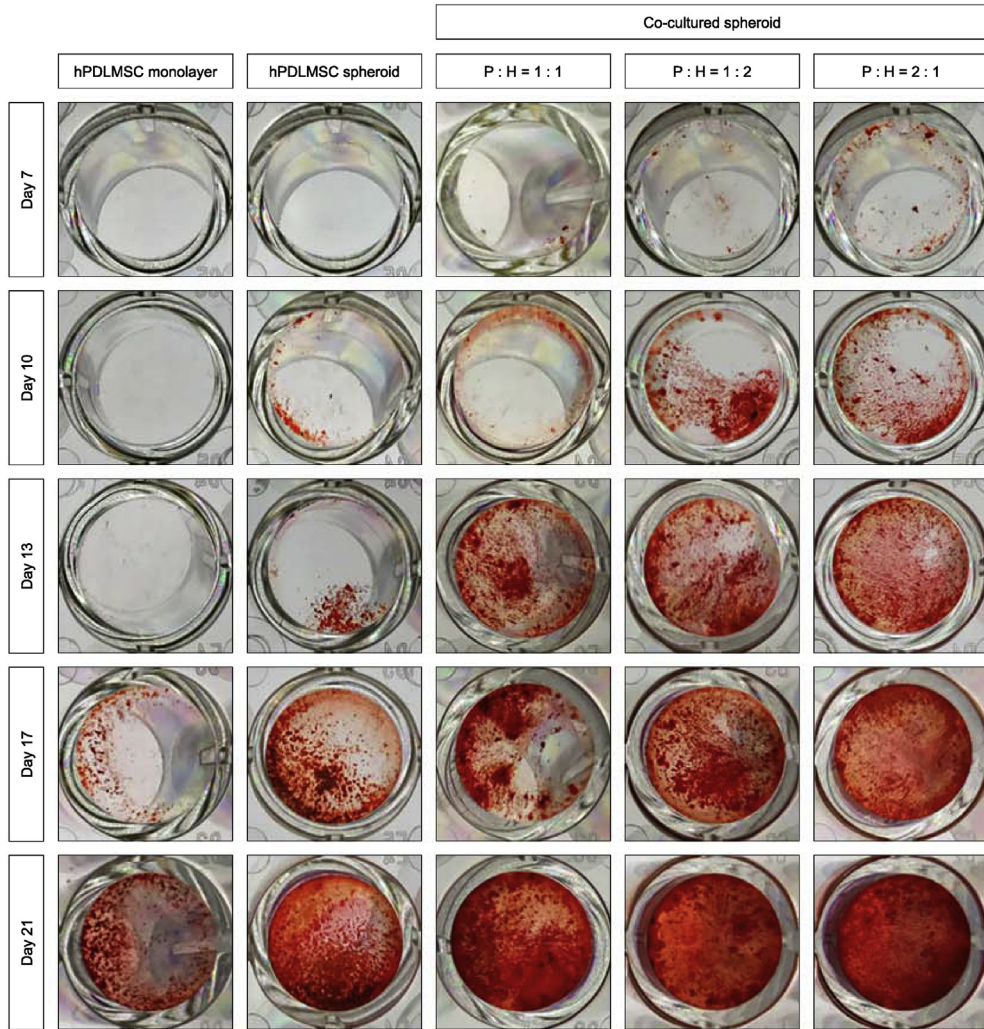
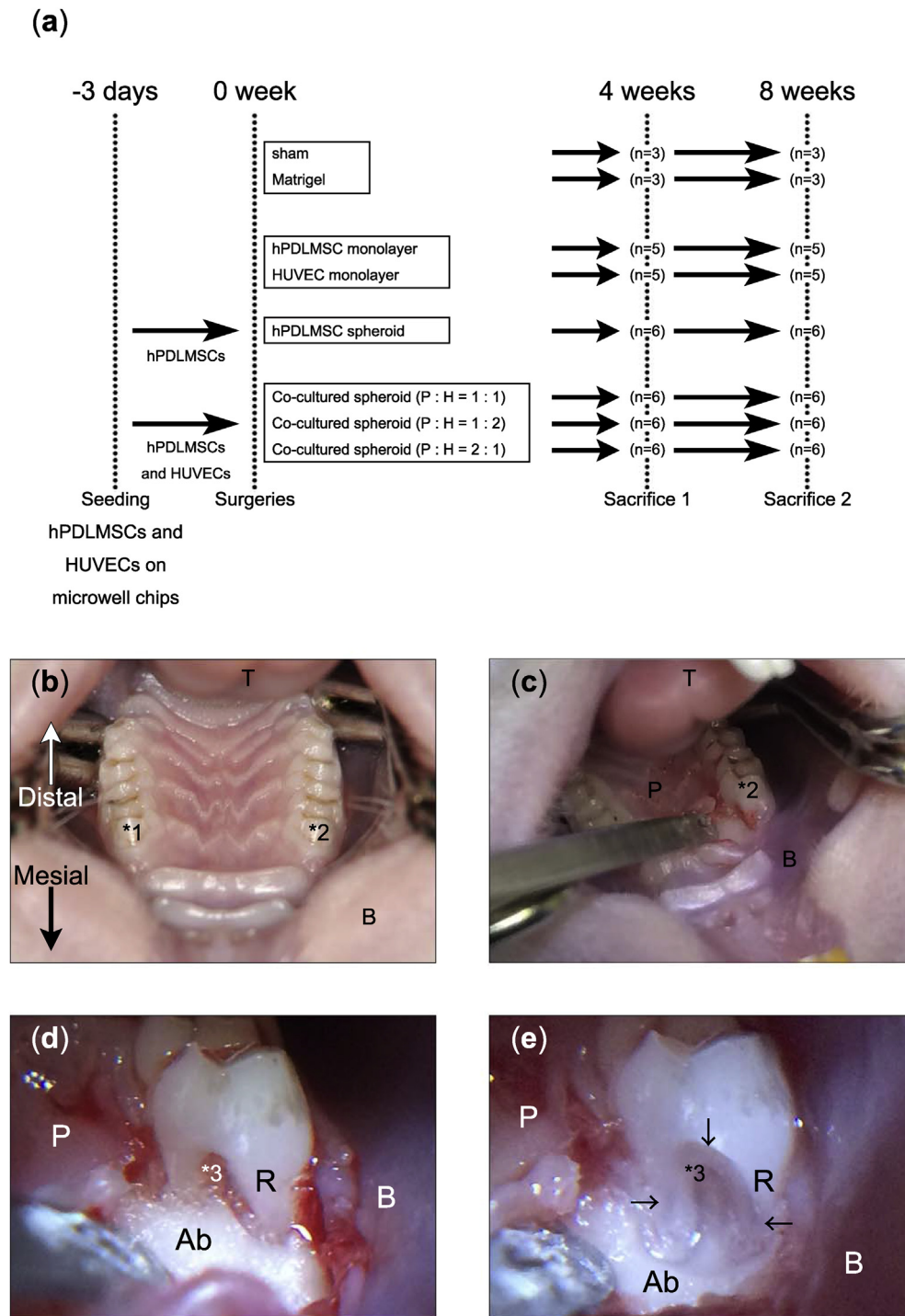**(b)**
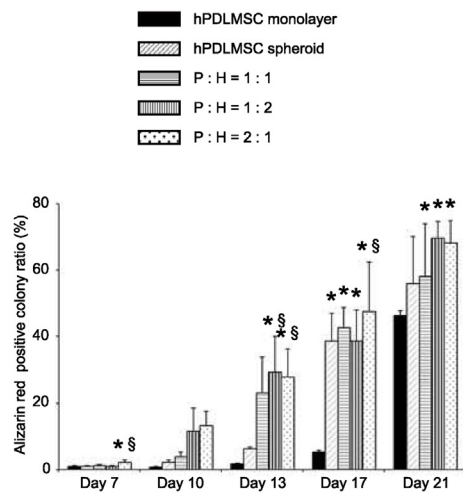
(c)

Fig. 3. Surgical creation of rat periodontal defects. (**a**) The study design of the transplantation assay. (**b**) Image of surgical field focused around rat maxilla. The surgical site was the bilateral maxillary first molar on the mesial furcation, as shown in *1 and *2. (**c**) Image during surgery. A full-thickness flap was raised and the alveolar bone was exposed around the right maxillary first molar. (**d, e**) Enlarged images of the operation area before creation of the defect (**d**) and after creation of the defect (**e**). *1, left maxillary first molar; *2, right maxillary first molar; *3, furcation of right maxillary first molar; T, tongue; B, buccal mucosa; P, palatal gingiva; Ab, alveolar bone; R, tooth root; arrow head, margin of defect.

Fig. 2. Enhancement of osteogenic differentiation in co-cultured spheroids *in vitro*. (**a**) Nodules formed by co-cultured spheroids, hPDLMSC spheroids, and monolayer-cultured hPDLMSCs at each time point. Co-cultured spheroids (cell ratio of hPDLMSCs: HUVEC = 1:1, 1:2, and 2:1), hPDLMSC spheroids, and monolayer-cultured hPDLMSCs were grown in 2D culture until confluent in α-MEM and/or EGM-2, and then incubated in OIM for 7, 10, 13, 17, or 21 days. Cells were stained with alizarin red. P, hPDLMSC; H, HUVEC. (**b**) Quantification of alizarin red-positive colonies (calcium deposits). $*p < 0.05$ (compared with monolayer cultures of hPDLMSCs). $\S p < 0.05$ (compared with hPDLMSC spheroids). (**c**) Expression of osteogenesis-related genes in co-cultured spheroids (1:1, 1:2, and 2:1), hPDLMSC spheroids, monolayer hPDLMSCs cultured in OIM on day 7, 10, and 14. The values were normalized to *GAPDH* expression. $*p < 0.05$ (compared with monolayer-cultured hPDLMSCs). $\S p < 0.05$ (compared with hPDLMSC spheroids).
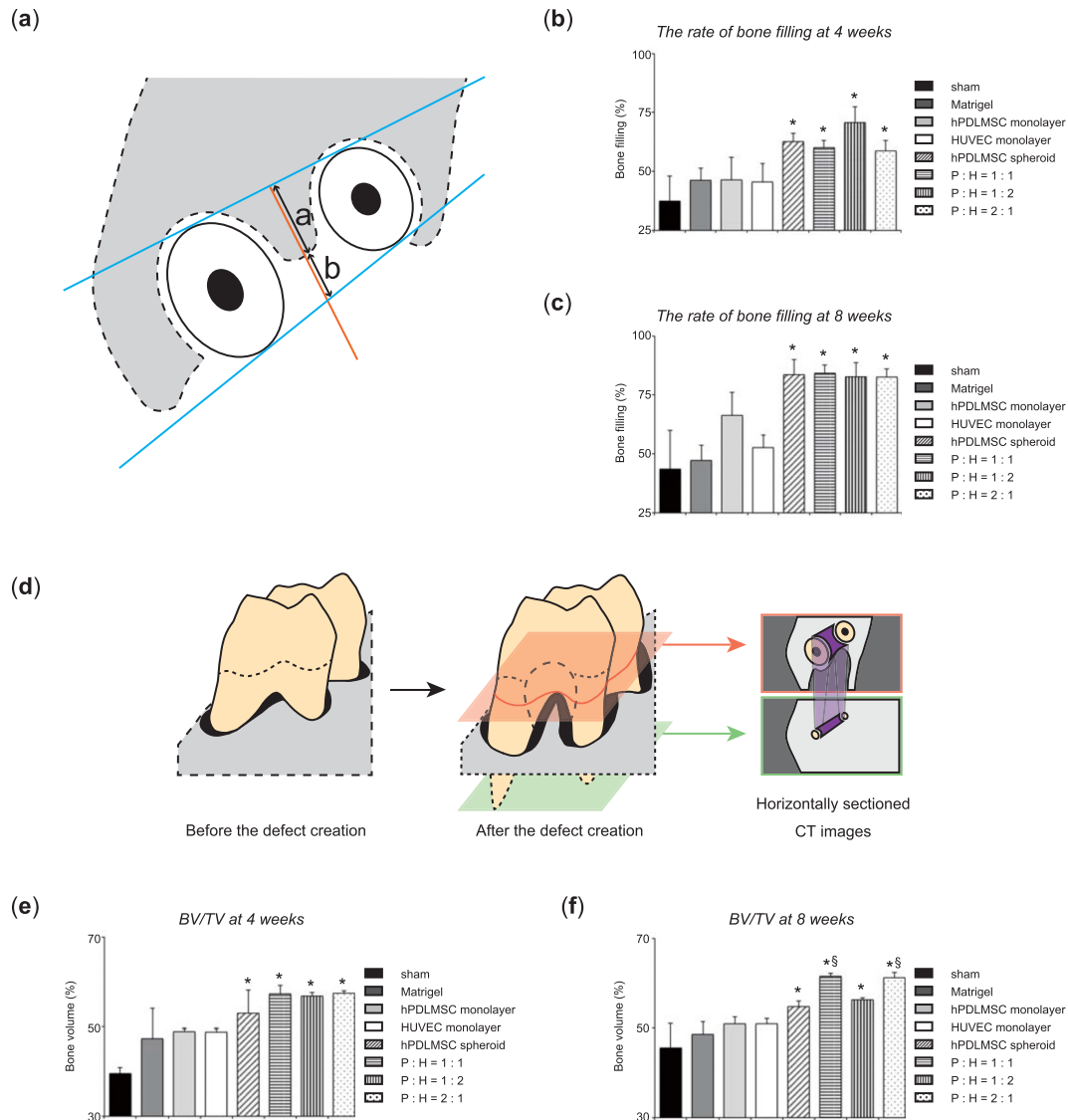
Fig. 4. New bone formation after transplantation of co-cultured spheroids, analyzed by 3D μCT. (**a**–**c**) Quantification of bone formation at the furcation in horizontally sectioned μCT images. (**a**) Schematic representation of parameters for measurement. Two tangent lines (blue) were drawn at the mesial and distal sides of the palatal and mesiobuccal roots. A perpendicular line (orange) was drawn on the distal tangent line at the center of the furcation. On the perpendicular line, the length from each tangent line to the bone margin (a and b) was measured. The rate of bone filling was calculated as (a/a+b) × 100. (**b**, **c**) The rate of bone filling at 4 weeks (**b**), and 8 weeks (**c**). *$p < 0.05$ (compared with sham). (**d**–**f**) Quantification of 3D bone formation at the furcation in 3D μCT images. (**d**) Schematic representation of parameters for measurement. BV/TV in the defect created at the mesial furcation (purple area in horizontally sectioned CT images) was measured from the plane including the mesial furcation surrounded with the mesiobuccal root and palatal root (red plane) to the plane including the root apex (green plane). (**e**, **f**) BV/TV at 4 weeks (**e**), and 8 weeks (**f**). *$p < 0.05$ (compared with sham). §$p < 0.05$ (compared with monolayer-cultured hPDLMSC).

spheroids (hPDLMSCs: HUVECs = 1:1, 1:2, and 2:1) and hPDLMSC spheroid groups (Fig. 6 (c)). In other words, connective tissue attachments occurred between the regenerated periodontal ligament fibers and new cementum. These data suggested that transplantation of co-cultured spheroids induced significantly new cementum formation and produced connective tissue attachments, compared with the formation induced in the hPDLMSC spheroid group.

Taken together, it was revealed that co-cultured spheroids formed more cementum than hPDLMSC spheroids, although there was no significant difference in osteogenesis between the groups treated with co-cultured spheroids and the group treated with hPDLMSC spheroid. To examine the mechanism behind this event, we examined the expression of *VEGF* mRNA and VEGF protein

secretion in co-cultured spheroids (hPDLMSCs: HUVECs = 1:1, 1:2, and 2:1), hPDLMSC spheroids, and monolayer-cultured hPDLMSCs and HUVECs by real-time RT-PCR and Enzyme-Linked Immuno Sorbent Assay (ELISA). The expression levels of VEGF were significantly higher in co-cultured spheroids (hPDLMSCs: HUVECs = 1:1 and 2:1) than in hPDLMSC spheroids (Fig. 6 (d), (e)). These data suggested that VEGF might be involved in cementogenesis by transplantation of co-cultured spheroids.

4. Discussion

Researches on periodontal tissue regeneration using MSCs have been conducted recently. The source of MSCs includes many tissues, such as bone marrow, adipose, and periosteal. MSCs isolated
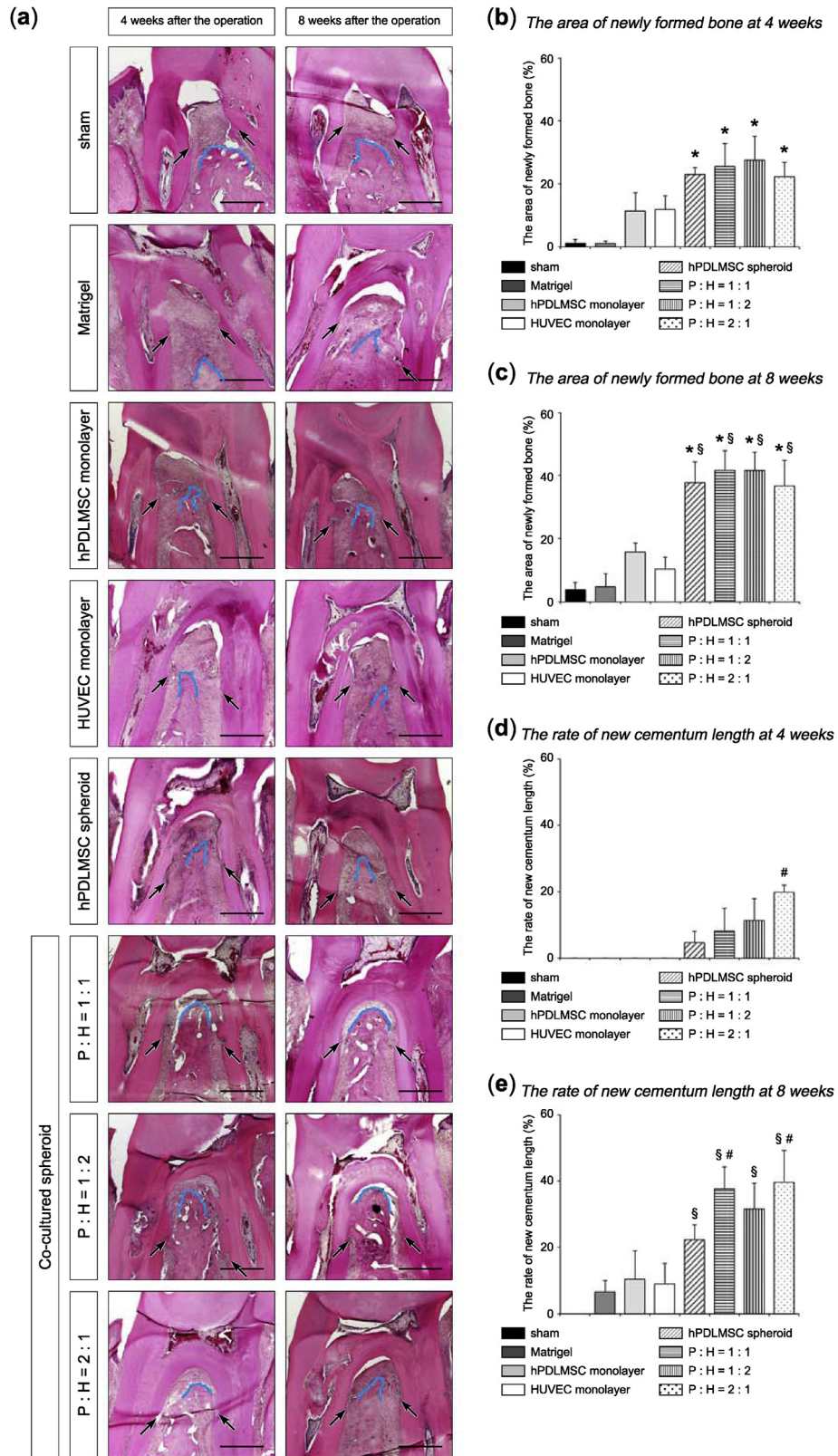
Fig. 5. Histological images focused on the formation of new bone and new cementum after transplantation of co-cultured spheroids. (**a**) H&E stained sections of the surgical sites in the rat maxillary first molar in each group. Black arrows indicate surgically created notches that show the bottom of the defects. Each blue line traces the coronal margin of the alveolar bone 4 or 8 weeks after transplantation. P, hPDLMSC; H, HUVEC. Scale bar = 500 μm. (**b, c**) Histomorphometric analysis of new bone formation. The areas of newly formed bone at 4 weeks (**b**), and 8 weeks (**c**) were calculated in each group. $^*p < 0.05$ (compared with sham). $^§p < 0.05$ (compared with monolayer-cultured hPDLMSCs). (**d, e**) Quantification of new cementum length. The rates of new cementum length at 4 weeks (**d**), and 8 weeks (**e**) were calculated in each group. $^§p < 0.05$ (compared with monolayer-cultured hPDLMSCs). $^#p < 0.05$ (compared with hPDLMSC spheroids).
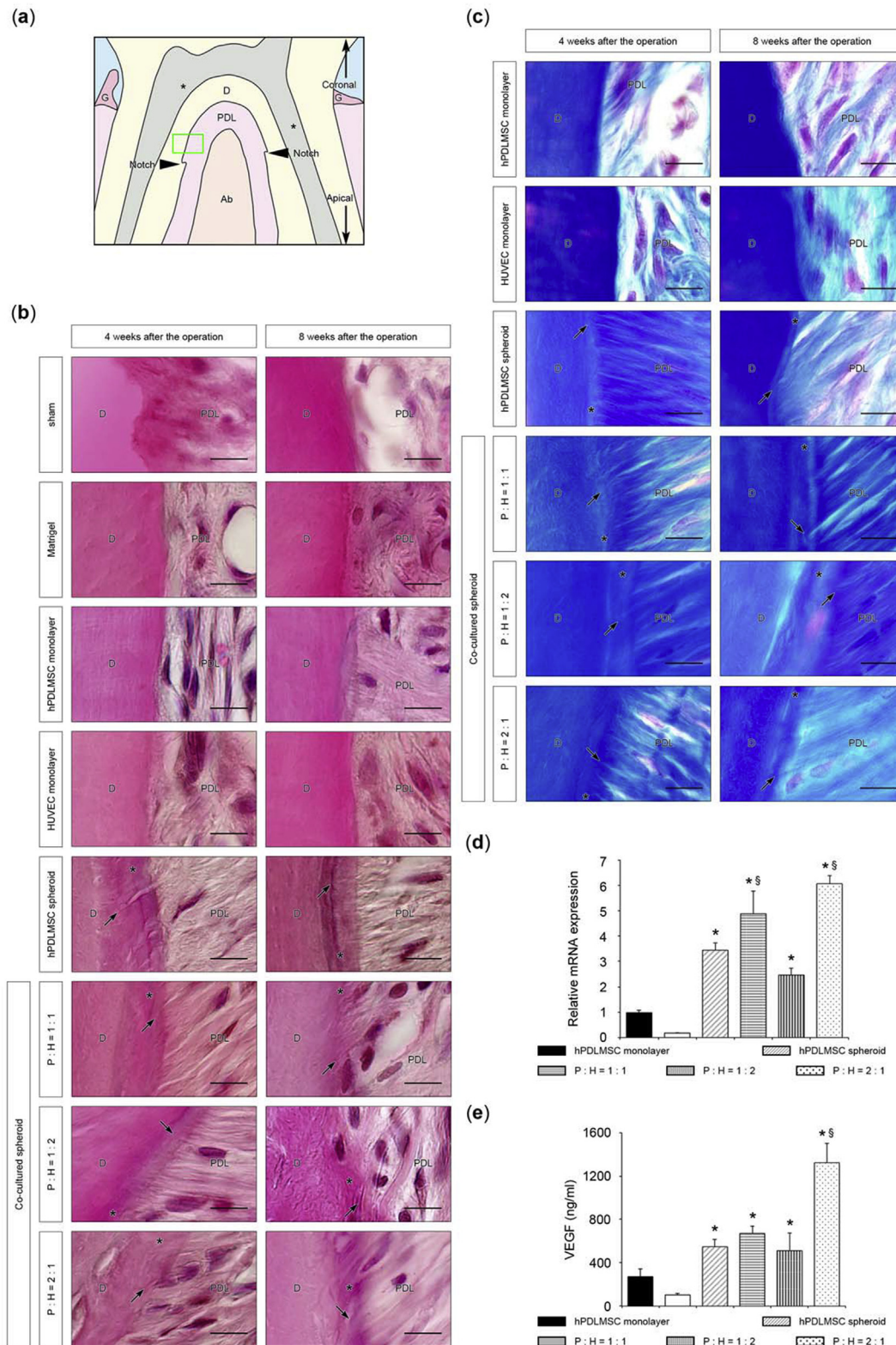
Fig. 6. Histological observation of Sharpey's fibers after transplantation of co-cultured spheroids. (**a**) Schematic representation of observed area at high magnification. In both H&E staining (**b**) and Azan staining (**c**), cementum was observed around the green frame, located 100 μm above the notch. PDL, periodontal ligament; D, dentin; asterisk, dental pulp; Ab, alveolar bone; G, gingiva. (**b**) Higher magnification images of periodontal tissues stained with H&E. Newly formed cementum layers (asterisk) were evident on spheroid (co-cultured, hPDLMSC)-transplanted root surface; therefore, Sharpey's fibers (black arrow) were observed on the spheroid (co-cultured, hPDLMSC)-transplanted cementum layers. P, hPDLMSC; H, HUVEC; asterisk, cementum; black arrows, Sharpey's fiber. Scale bar = 10 μm. (**c**) Azan staining of periodontal tissues in cell transplant groups with high magnification. Scale bar = 10 μm. (**d**) Expression of *VEGF* in co-cultured spheroids (cell ratio of hPDLMSCs: HUVECs = 1:1, 1:2, and 2:1), hPDLMSC spheroids, hPDLMSCs and HUVECs grown in monolayer culture on day 3. The values were normalized to *GAPDH* expression. *$p < 0.05$ (compared with monolayer-cultured hPDLMSCs). §$p < 0.05$ (compared with hPDLMSC spheroids). (**e**) The protein levels of VEGF in the supernatant determined by ELISA. The data represent the means ± SD of triplicate assays. *$p < 0.05$ (compared with monolayer-cultured hPDLMSCs). §$p < 0.05$ (compared with hPDLMSC spheroids).

from ilium and adipose tissue-derived stem cells induced periodontal tissue regeneration in a canine model [31,33]. Tsumanuma et al. [11] transplanted cell sheets derived from three types of mesenchymal tissues (periodontal ligament, alveolar periosteum, and bone marrow) into the canine periodontal defect models, and compared the effects of cell sources on the regeneration. Consequently, they have concluded that the amount of newly formed cementum and alveolar bone was the highest in the periodontal ligament MSC cell sheet group. In addition, they examined the safety and efficacy of allogeneic transplantation of PDLMSC sheets with a canine periodontal defect model, and PDLMSC sheets could promote periodontal tissue regeneration in both the autologous and the allogeneic transplantation groups [12]. These data suggested that, PDLMSCs are superior for periodontal tissue regeneration among MSCs and suitable for clinical application. Thus, we investigated the effect of spheroid culture of hPDLMSCs, and showed that spheroid culture enhanced stemness of hPDLMSCs, and osteogenic potential of hPDLMSCs cultured in OIM [17]. On the other hand, some studies examined the effect of combining MSCs with other cells. Pandula et al. [26] have shown that a hPDLMSC–HUVEC co-cultured cell sheet exhibited significantly high levels of osteogenesis-related markers, compared with monocultures of hPDLMSCs. In this study, we evaluated the periodontal regenerative potential of co-cultured spheroids prepared by 3D culture of hPDLMSCs and vascular endothelial cells.

We generated co-cultured spheroids with microwell chips and revealed that the expression of stemness markers (OCT4 and NANOG) was enhanced by co-culture with hPDLMSCs: HUVECs at a ratio of 1:2. The expression of OCT4 and NANOG was up-regulated in co-culture of endothelial progenitor cells (EPCs) and MSCs using indirect Transwell co-culture system, compared with mono-cultured MSCs [34]. In addition, some researchers showed that the expression of microRNA 489 (miR-489), which had been reported to greatly involve in regulation of the stem cell quiescence, was significantly increased in spheroid-cultured human MSCs (hMSCs), compared with monolayer-cultured hMSCs [35,36]. These results suggested that co-cultured spheroids restored their stem cell properties through a quiescent status of hPDLMSCs. Therefore, some other factors produced from HUVECs may enhance stemness of co-cultured spheroids.

We have confirmed the high expression levels of osteogenesis-related genes in co-cultured spheroids that were exposed to osteogenic differentiation conditions. This result was consistent with the previous report that osteogenesis-related genes were highly expressed in the cell sheets co-cultured with hPDLMSCs and HUVECs, compared with hPDLMSC cell sheets [24]. Wen et al. [34] have reported that MSCs co-cultured with EPCs significantly increased gene and protein levels of OCN, BSP, and RUNX2, compared with monocultured MSCs. HUVEC produces VEGF that has a paracrine effect and promotes MSCs to osteogenic differentiation [37,38]. In this study, we confirmed that VEGF gene and protein levels were elevated in co-cultured spheroids. These findings suggested that HUVEC-derived paracrine factors might enhance the osteogenic potential of hPDLMSCs. Although 1:1 and 2:1 (hPDLMSCs: HUVECs) co-cultured spheroids regenerated more bone volume in periodontal tissue defect model compared with other groups, osteogenesis-related gene expression in 1:2 (hPDLMSCs: HUVECs) co-cultured spheroids was the highest among spheroid groups in vitro. The data of newly bone formation in vivo is not completely consistent with enhancement of osteogenesis-related genes in vitro due to the difference in the ratio between hPDLMSCs and HUVECs. Since in vitro is a closed system, VEGF from HUVECs would enhance the osteogenic potential of hPDLMSCs directly. On the other hands, various cytokines and growth factors derived from many kinds of cells in periodontal

tissues other than co-cultured spheroids may take part in regeneration of alveolar bone in rat periodontal defect model.

To regenerate large tissues such as human tissues by MSC transplantation, a large number of stem cells would be required. Since it is difficult to collect large amounts of stem cells for autologous transplantation, it is necessary to perform repeated passages of stem cells. However, successive passages of human stem cells impair their osteogenic potential, and these cells may be inappropriate for clinical application [39]. Moreover, monolayer cultures of hMSCs in late passages have been reported to trigger spontaneous differentiation and signs of aging, such as declined potential for multipotent differentiation and tissue repair [40,41]. Spheroid culture with our microwell chip may restore undifferentiated state and pluripotent ability of stem cells lost by monolayer culture because the microwell chip we used in this study enhanced the gene and protein expression of OCT4 and NANOG in hPDLMSCs [17]. It is a topic to examine the detailed mechanism of spheroid culture in the future.

The new bone formation was augmented in the defects after transplantation with co-cultured spheroids, as well as hPDLMSC spheroids transplanted groups. In contrast, the new cementum formation in the co-cultured spheroid groups was significantly higher than that in hPDLMSCs spheroid group. It has been reported that functional tissue attachment occurs in the cementum where Sharpey's fibers enter, so it is known that the presence of Sharpey's fibers and newly formed cementum is essential for periodontal regeneration [11]. We examined that Sharpey's fibers of the regenerated periodontal ligament entered in newly formed cementun. Considering the mechanisms involved in new cementum formation, it can also be assumed that transplanted hPDLMSCs directly differentiate into cementoblasts. Although close contact between recipient site and transplanted cells is necessary in the periodontal tissues, it may be difficult to achieve tight contact between recipient site and transplanted cells in the case of using scaffold materials, such as collagen gels. According to microscopy observations, newly formed cementum was successively generated from the edge of the defects (notch), and there was no newly formed cementum which was not along the host tissue and scattered in the defect sites. These findings suggested that new cementum formation occurred from the host (rat) tissue just below the notches. Therefore, we consider that periodontal regeneration was promoted by the cells derived from host (rat) tissues, and differences in alveolar bone and cementum regeneration are due to the factors produced by transplanted cells or the production of the factors.

From the viewpoint of future clinical applications of cell transplantation, it is necessary to consider the appropriate number of transplanted cells or spheroids and population of hPDLMSCs and HUVECs. This study revealed that periodontal tissue defect ($1.3 \times 1.3 \times 1.0$ mm) was regenerated by 200 co-cultured spheroids (2000 cells/spheroid). Although MSCs or hPDLMSCs transplantations have been performed for bone defects and periodontal tissue defects in many studies, the size of the defects, the number of transplanted cells, the number of cells per defect volume and scaffold of cells are different [11,12,42]. Currently, there is no clear indication of the number of transplanted MSCs and the scaffold required per defect volume of periodontal defect. Based on this study, it is necessary to examine in detail the appropriate transplanted cell numbers including spheroids, population of hPDLMSCs and HUVECs and scaffold for regenerating the periodontal tissue defects for the future analysis.

We elucidated that the gene expression level of VEGF and VEGF protein levels in supernatants were significantly higher in co-cultured spheroids (hPDLMSCs: HUVECs = 1:1 and 2:1) than in

hPDLMSC spheroids. We assumed that VEGF from co-cultured spheroids would enhance the differentiation into cementoblasts and the formation of cementum. The precise mechanisms by which co-cultured spheroids enhance periodontal tissue formation remain unclear. Further studies are underway to clarify these points.

5. Conclusions

In this study, we have shown that co-cultured spheroids significantly enhanced cementum formation in rat periodontal tissue defects, compared with both monolayer and spheroid-cultured hPDLMSCs. These data suggested that co-cultured spheroid might be a promising method for periodontal regeneration.

Author contributions

K.S. mainly performed the experiments, analyzed the data, and wrote the manuscript. M.U. designed the project and provided funding and supervision; in addition, he was a major contributor in drafting the manuscript. Y.M. contributed to establishment of the protocol for preparing spheroids using microwell chips. K.N. provided microwell chips. T.H. provided funding and gave *in vivo* technical guidance. H.K. and A.T. assisted in 3D μCT analysis and interpretation of data. M.N. assisted in histological acquisition and evaluation of data. S.O. provided feedback and critically revised. T.I. and T.S. provided the conceptual framework for the study. W.A. and T.N. also provided suggestions and feedback. K.N. provided feedback and supervision. All authors contributed to the writing, and have approved the final manuscript.

Declaration of Competing interest

The authors declare no competing interests.

References

[1] Pihlstrom BL, Michalowicz BS, Johnson NW. Periodontal diseases. Lancet 2005;366:1809—20.
[2] Murakami S. Periodontal tissue regeneration by signaling molecule(s): what role does basic fibroblast growth factor (FGF-2) have in periodontal therapy? Periodontol 2000 2011;56:188—208.
[3] Van Dyke TE, Hasturk H, Kantarci A, Freire MO, Nguyen D, Dalli J, et al. Pro-resolving nanomedicines activate bone regeneration in periodontitis. J Dent Res 2015;94:148—56.
[4] Kitamura M, Akamatsu M, Kawanami M, Furuichi Y, Fujii T, Mori M, et al. Randomized placebo-controlled and controlled non-inferiority phase III trials comparing trafermin, a recombinant human fibroblast growth factor 2, and enamel matrix derivative in periodontal regeneration in intrabony defects. J Bone Miner Res 2016;31:806—14.
[5] Pittenger MF, Mackay AM, Beck SC, Jaiswal RK, Douglas R, Mosca JD, et al. Multilineage potential of adult human mesenchymal stem cells. Science 1999;284:143—7.
[6] Liu ZJ, Zhuge Y, Velazquez OC. Trafficking and differentiation of mesenchymal stem cells. J Cell Biochem 2009;106:984—91.
[7] Seo BM, Miura M, Gronthos S, Bartold PM, Batouli S, Brahim J, et al. Investigation of multipotent postnatal stem cells from human periodontal ligament. Lancet 2004;364:149—55.
[8] Nagatomo K, Komaki M, Sekiya I, Sakaguchi Y, Noguchi K, Oda S, et al. Stem cell properties of human periodontal ligament cells. J Periodontal Res 2006;41:303—10.
[9] Iwata T, Yamato M, Zhang Z, Mukobata S, Washio K, Ando T, et al. Validation of human periodontal ligament-derived cells as a reliable source for cytotherapeutic use. J Clin Periodontol 2010;37:1088—99.
[10] Nojima N, Kobayashi M, Shionome M, Takahashi N, Suda T, Hasegawa K. Fibroblastic cells derived from bovine periodontal ligaments have the phenotypes of osteoblasts. J Periodontal Res 1990;25:179—85.
[11] Tsumanuma Y, Iwata T, Washio K, Yoshida T, Yamada A, Takagi R, et al. Comparison of different tissue-derived stem cell sheets for periodontal regeneration in a canine 1-wall defect model. Biomaterials 2011;32:5819—25.
[12] Tsumanuma Y, Iwata T, Kinoshita A, Washio K, Yoshida T, Yamada A, et al. Allogeneic transplantation of periodontal ligament-derived multipotent mesenchymal stromal cell sheets in canine critical-size supra-alveolar periodontal defect model. Biores Open Access 2016;5:22—36.
[13] Yamada N, Okano T, Sakai H, Karikusa F, Sawasaki Y, Sakurai Y. Thermoresponsive polymeric surfaces; control of attachment and detachment of cultured cells. Die Makromol Chem Rapid Comm 1990;11:571—6.
[14] Koike M, Sakaki S, Amano Y, Kurosawa H. Characterization of embryoid bodies of mouse embryonic stem cells formed under various culture conditions and estimation of differentiation status of such bodies. J Biosci Bioeng 2007;104:294—9.
[15] Lazar A, Mann HJ, Remmel RP, Shatford RA, Cerra FB, Hu WS. Extended liver-specific functions of porcine hepatocyte spheroids entrapped in collagen gel. Vitro Cell Dev Biol Anim 1995;31:340—6.
[16] Haycock JW. 3D cell culture: a review of current approaches and techniques. Methods Mol Biol 2011;695:1—15.
[17] Moritani Y, Usui M, Sano K, Nakazawa K, Hanatani T, Nakatomi M, et al. Spheroid culture enhances osteogenic potential of periodontal ligament mesenchymal stem cells. J Periodontal Res 2018;53:870—82.
[18] Rutherford RB, Moalli M, Franceschi RT, Wang D, Gu K, Krebsbach PH. Bone morphogenetic protein-transduced human fibroblasts convert to osteoblasts and form bone in vivo. Tissue Eng 2002;8:441—52.
[19] Wiesmann HP, Nazer N, Klatt C, Szuwart T, Meyer U. Bone tissue engineering by primary osteoblast-like cells in a monolayer system and 3-dimensional collagen gel. J Oral Maxillofac Surg 2003;61:1455—62.
[20] Cheng NC, Wang S, Young TH. The influence of spheroid formation of human adipose-derived stem cells on chitosan films on stemness and differentiation capabilities. Biomaterials 2012;33:1748—58.
[21] Yamamoto M, Kawashima N, Takashino N, Koizumi Y, Takimoto K, Suzuki N, et al. Three-dimensional spheroid culture promotes odonto/osteoblastic differentiation of dental pulp cells. Arch Oral Biol 2014;59:310—7.
[22] Petrenko Y, Syková E, Kubinová S. The therapeutic potential of three-dimensional multipotent mesenchymal stromal cell spheroids. Stem Cell Res Ther 2017;8:94.
[23] Wang W, Itaka K, Ohba S, Nishiyama N, Chung UI, Yamasaki Y, et al. 3D spheroid culture system on micropatterned substrates for improved differentiation efficiency of multipotent mesenchymal stem cells. Biomaterials 2009;30:2705—15.
[24] Sakai Y, Nakazawa K. Technique for the control of spheroid diameter using microfabricated chips. Acta Biomater 2007;3:1033—40.
[25] Sakai Y, Yoshida S, Yoshiura Y, Mori R, Tamura T, Yahiro K, et al. Effect of microwell chip structure on cell microsphere production of various animal cells. J Biosci Bioeng 2010;110:223—9.
[26] Pandula PK, Samaranayake LP, Jin LJ, Zhang CF. Human umbilical vein endothelial cells synergize osteo/odontogenic differentiation of periodontal ligament stem cells in 3D cell sheets. J Periodontal Res 2014;49:299—306.
[27] Panduwawala CP, Zhan X, Dissanayaka WL, Samaranayake LP, Jin L, Zhang C. In vivo periodontal tissue regeneration by periodontal ligament stem cells and endothelial cells in three-dimensional cell sheet constructs. J Periodontal Res 2017;52:408—18.
[28] Onizuka S, Iwata T, Park SJ, Nakai K, Yamato M, Okano T, et al. ZBTB16 as a downstream target gene of osterix regulates osteoblastogenesis of human multipotent mesenchymal stromal cells. J Cell Biochem 2016;117:2423—34.
[29] Usui M, Sato T, Yamamoto G, Okamatsu Y, Hanatani T, Moritani Y, et al. Gingival epithelial cells support osteoclastogenesis by producing receptor activator of nuclear factor kappa B ligand via protein kinase A signaling. J Periodontal Res 2015;51:462—70.
[30] Iwasaki K, Komaki M, Yokoyama N, Tanaka Y, Taki A, Honda I, et al. Periodontal regeneration using periodontal ligament stem cell-transferred amnion. Tissue Eng Part A 2014;20:693—704.
[31] Takewaki M, Kajiya M, Takeda K, Sasaki S, Motoike S, Komatsu N, et al. MSC/ECM cellular complexes induce periodontal tissue regeneration. J Dent Res 2017;96:984—91.
[32] Nagahara T, Yoshimatsu S, Shiba H, Kawaguchi H, Takeda K, Iwata T, et al. Introduction of a mixture of β-tricalcium phosphate into a complex of bone marrow mesenchymal stem cells and type I collagen can augment the volume of alveolar bone without impairing cementum regeneration. J Periodontol 2015;86:456—64.
[33] Tobita M, Uysal CA, Guo X, Hyakusoku H, Mizuno H. Periodontal tissue regeneration by combined implantation of adipose tissue-derived stem cells and platelet-rich plasma in a canine model. Cytotherapy 2013;15:1517—26.
[34] Wen L, Wang Y, Wen N, Yuan G, Wen M, Zhang L, et al. Role of endothelial progenitor cells in maintaining stemness and enhancing differentiation of

mesenchymal stem cells by indirect cell-cell interaction. Stem Cells Dev 2016;25:123–38.

[35] Guo L, Zhou Y, Wang S, Wu Y. Epigenetic changes of mesenchymal stem cells in three-dimensional (3D) spheroids. J Cell Mol Med 2014;18:2009–19.

[36] Cheung TH, Quach NL, Charville GW, Liu L, Park L, Edalati A, et al. Maintenance of muscle stem-cell quiescence by microRNA-489. Nature 2012;482:524–8.

[37] Imaizumi T, Itaya H, Nasu S, Yoshida H, Matsubara Y, Fujimoto K, et al. Expression of vascular endothelial growth factor in human umbilical vein endothelial cells stimulated with interleukin-1alpha–an autocrine regulation of angiogenesis and inflammatory reactions. Thromb Haemost 2000;83: 949–55.

[38] Berendsen AD, Olsen BR. How vascular endothelial growth factor-A (VEGF) regulates differentiation of mesenchymal stem cells. J Histochem Cytochem 2014;62:103–8.

[39] Di Battista JA, Shebaby W, Kizilay O, Hamade E, Abou Merhi R, Mebarek S, et al. Proliferation and differentiation of human adipose-derived mesen-chymal stem cells (ASCs) into osteoblastic lineage are passage dependent. Inflamm Res 2014;63:907–17.

[40] Krampera M, Pasini A, Rigo A, Scupoli MT, Tecchio C, Malpeli G, et al. HB-EGF/ HER-1 signaling in bone marrow mesenchymal stem cells: inducing cell expansion and reversibly preventing multilineage differentiation. Blood 2005;106:59–66.

[41] Li Z, Liu C, Xie Z, Song P, Zhao RC, Guo L, et al. Epigenetic dysregulation in mesenchymal stem cell aging and spontaneous differentiation. PLoS One 2011. https://doi.org/10.1371/journal.pone.0020526.

[42] Yamaguchi Y, Ohno J, Sato A, Kido H, Fukushima T. Mesenchymal stem cell spheroids exhibit enhanced in-vitro and in-vivo osteoregenerative potential. BMC Biotechnol 2014;14:105.